



The Prognostic Significance and Potential Mechanism of Ferroptosis-Related Genes in Hepatocellular Carcinoma

Wenli Li¹, Jun Liu², Dangui Zhang³, Liming Gu^{4,5*†} and Hetong Zhao^{6*†}

OPEN ACCESS

Edited by:

Xuekui Zhang,
University of Victoria, Canada

Reviewed by:

Zaoqu Liu,
First Affiliated Hospital of Zhengzhou
University, China
Jianni Qi,
Shandong Provincial Hospital Affiliated
to Shandong First Medical University,
China

*Correspondence:

Liming Gu
13lmgu@stu.edu.cn
Hetong Zhao
zhtzhao@126.com

[†]These authors have contributed
equally to this work

Specialty section:

This article was submitted to
Computational Genomics,
a section of the journal
Frontiers in Genetics

Received: 28 December 2021

Accepted: 24 March 2022

Published: 26 April 2022

Citation:

Li W, Liu J, Zhang D, Gu L and Zhao H
(2022) The Prognostic Significance
and Potential Mechanism of
Ferroptosis-Related Genes in
Hepatocellular Carcinoma.
Front. Genet. 13:844624.
doi: 10.3389/fgene.2022.844624

¹Reproductive Medicine Center, Yue Bei People's Hospital, Shantou University Medical College, Shaoguan, China, ²Medical Research Center, Yue Bei People's Hospital, Shantou University Medical College, Shaoguan, China, ³Research Center of Translational Medicine, Second Affiliated Hospital of Shantou University Medical College, Shantou, China, ⁴Guangdong Provincial Key Laboratory of Infectious Diseases and Molecular Immunopathology, Shantou University Medical College, Shantou, China, ⁵Department of Microbiology and Immunology, Center of Pathogen Biology and Immunology, Shantou University Medical College, Shantou, China, ⁶Department of Traditional Chinese Medicine, Navy NO.905 Hospital, Naval Military Medical University, Shanghai, China

Ferroptosis exerts a pivotal role in the formation and dissemination processes of hepatocellular carcinoma (HCC). The heterogeneity of ferroptosis and the link between ferroptosis and immune responses have remained elusive. Based on ferroptosis-related genes (FRGs) and HCC patients from The Cancer Genome Atlas (TCGA), International Cancer Genome Consortium (ICGC), and Gene Expression Omnibus (GEO) cohorts, we comprehensively explored the heterogeneous ferroptosis subtypes. The genetic alterations, consensus clustering and survival analysis, immune infiltration, pathway enrichment analysis, integrated signature development, and nomogram building were further investigated. Kaplan–Meier plotter confirmed statistically differential probabilities of survival among the three subclusters. Immune infiltration analysis showed there were clear differences among the types of immune cell infiltration, the expression of PD-L1, and the distribution of TP53 mutations among the three clusters. Univariate Cox regression analysis, random survival forest, and multivariate Cox analysis were used to identify the prognostic integrated signature, including MED8, PIGU, PPM1G, RAN, and SNRPB. Kaplan–Meier analysis and time-dependent receiver operating characteristic (ROC) curves revealed the satisfactory predictive potential of the five-gene model. Subsequently, a nomogram was established, which combined the signature with clinical factors. The nomogram including the ferroptosis-based signature was conducted and showed some clinical net benefits. These results facilitated an understanding of ferroptosis and immune responses for HCC.

Keywords: ferroptosis, immune, hepatocellular carcinoma, prognosis, risk model

INTRODUCTION

Hepatocellular carcinoma (HCC) is a common and highly lethal disease around the world (Kulik and El-Serag, 2019). However, high recurrence rates after resection compromise patient outcomes (Tabrizian et al., 2015). Sorafenib and lenvatinib have been approved as first-line therapy for advanced HCC patients with clinical benefits and depend on ferroptosis to fulfill their cytotoxic effects (Llovet et al., 2008; Louandre et al., 2013; Kudo et al., 2018). Sorafenib can induce ferroptosis, and ferroptosis is involved in sorafenib resistance (Li et al., 2020). Further understanding of the molecular mechanism of ferroptosis may aid in developing new therapy for sorafenib resistance (Sun et al., 2016). Immune-based therapies are emerging as promising strategies to treat HCC patients (Hilmi et al., 2019). Triggering immune response is a promising feature of ferroptosis in immune-based therapies (Gorgen et al., 2020). However, the role and potential mechanisms of ferroptosis in the immune response of HCC still remain elusive.

Ferroptosis is considered an iron-dependent, non-apoptotic type of cell death which is associated with reactive oxygen species (ROS) (Li et al., 2020). Recent research has shown that ferroptosis is involved in the pathological processes of a number of diseases (Sun et al., 2016; Capelletti et al., 2020). Many ferroptosis regulators have been reported in certain cancer cells. For example, circRNA IARS could positively regulate ferroptosis by suppressing the ALKBH5-mediated autophagy inhibition in

HCC cells (Liu et al., 2020). A recent report also suggested that targeting ferroptosis could be a new promising strategy to improve sorafenib therapy (Nie et al., 2018). For instance, glutathione S-transferase zeta 1 enhanced sorafenib-induced ferroptosis in HCC cells (Wang Q. et al., 2021). Thus, further studies on the relationship between ferroptosis-related genes and HCC prognosis are needed.

In this study, we utilized publicly available gene expression datasets. Then, we revealed three distinct ferroptosis-related patterns, and these three patterns presented significant differences in immune cell infiltration and tumor mutations burden, suggesting that the ferroptosis-related genes exert a central role in the generation of the tumor immune microenvironment. Finally, we further constructed a five-gene signature to quantify the ferroptosis-related pattern in individual patients.

MATERIALS AND METHODS

Data Acquisition

The gene expression microarray and corresponding clinical information were acquired from The Cancer Genome Atlas-Liver Hepatocellular Carcinoma (TCGA-LIHC, <https://cancergenome.nih.gov/>). To validate the prognostic potential of the genetic risk score, the independent HCC datasets were obtained through the International Cancer Genome Consortium (ICGC, <https://icgc.org>) and the Gene Expression Omnibus

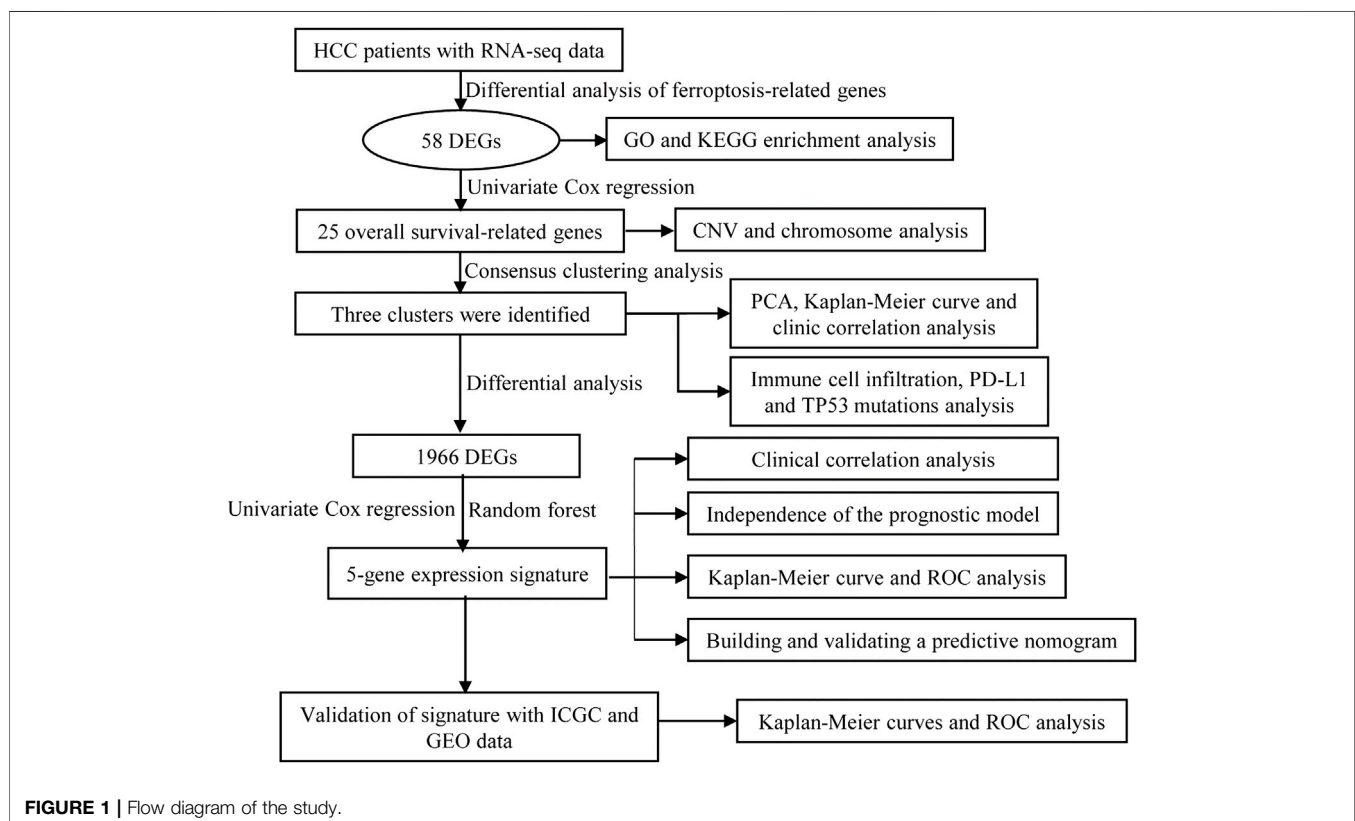
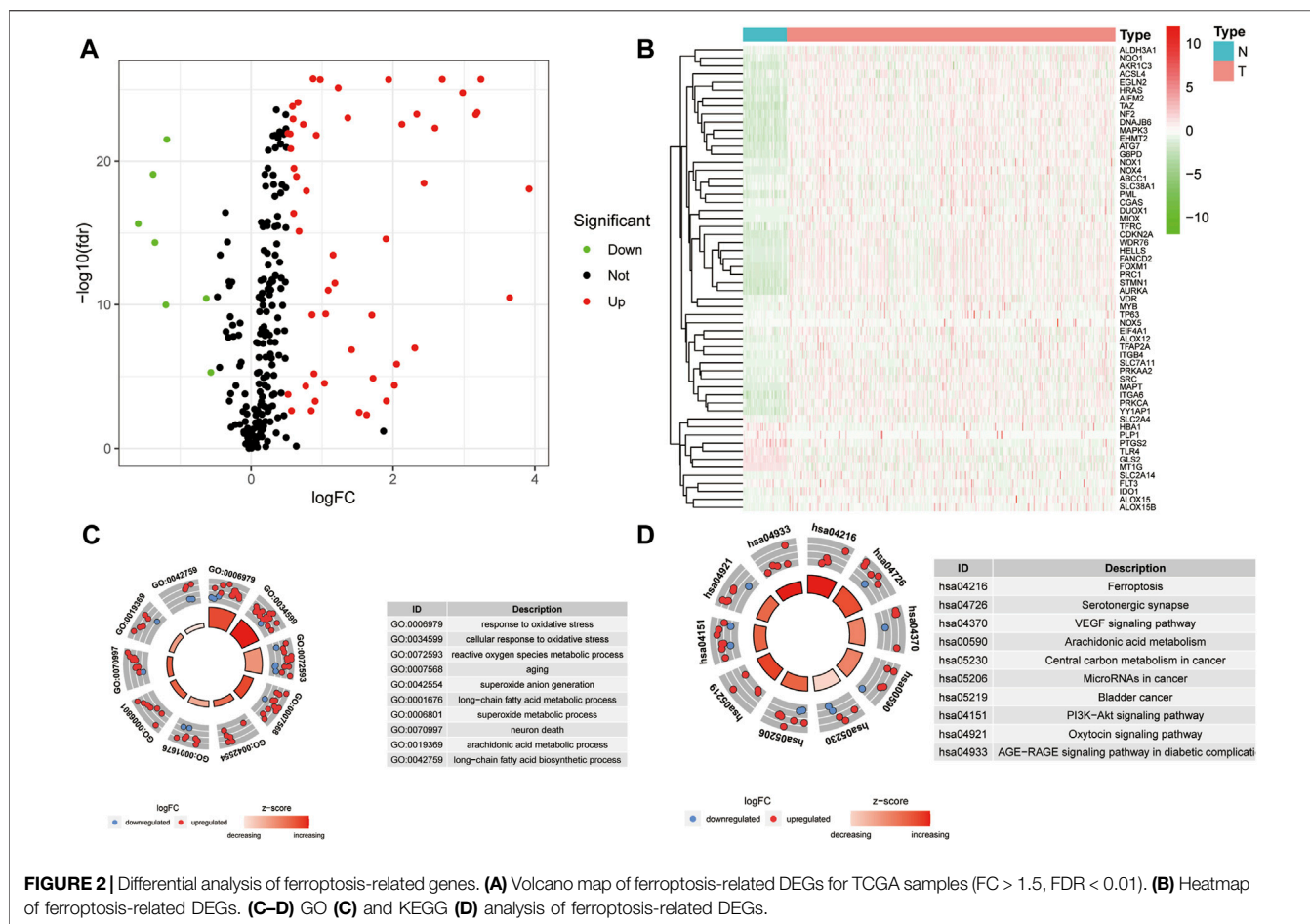


FIGURE 1 | Flow diagram of the study.



(GEO) database (GSE14520, Affymetrix HT Human Genome U133A Array, GPL3921). The protein expression profiles of HCC were acquired from The National Cancer Institute’s Clinical Proteomic Tumor Analysis Consortium (CPTAC, <https://cptac-data-portal.georgetown.edu/>). The ferroptosis-related genes (FRGs) were acquired from the FerrDb website (<http://www.zhounan.org/ferrdb>). All statistical analyses were performed in R version 4.0.5.

Identification of Differentially Expressed Genes

Differentially expressed genes (DEGs) were determined using R package “limma” (Ritchie et al., 2015) based on the comparison of gene expression levels between HCC and liver tissues in TCGA cohort. The selection criteria for identification of DEGs were as follows: $|\logFC| > 1$ and adjusted $p < 0.01$. This study fully complies with TCGA publication requirements (<http://cancergenome.nih.gov/publications/publicationguidelines>). Kaplan–Meier survival analysis and the Cox proportional hazards model were used to analyze the association between the different clusters and prognosis with the R package “Survminer.” The receiver operating characteristic (ROC) curve was used to assess the prognosis

classification performance of the signature and nomogram, and the area under the curve (AUC) was calculated using R package “timeROC.”

Functional Enrichment Analysis

The R package “clusterProfiler” was used for Gene Ontology (GO) and KEGG pathway analysis (Yu et al., 2012). $p < 0.01$ and $FDR < 0.05$ were considered statistically significant. Gene set enrichment analysis (GSEA) of hallmark gene sets was acquired from MSigDB database v7.1 (Hänzelmann et al., 2013; Subramanian et al., 2005).

Mutation Analysis

The genomic mutation data were curated from TCGA database. The copy number variation distribution information of FRGs on different chromosomes was plotted using the R package “Rcircos.”

Subclusters and PCA Analysis

To study the function of DEGs, we separated patients into three subclusters by the R package of “ConsensusClusterPlus” (Wilkerson and Hayes, 2010). The R package “ggplot2” of principal component analysis (PCA) was carried out to explore the genes in subclusters of HCC.

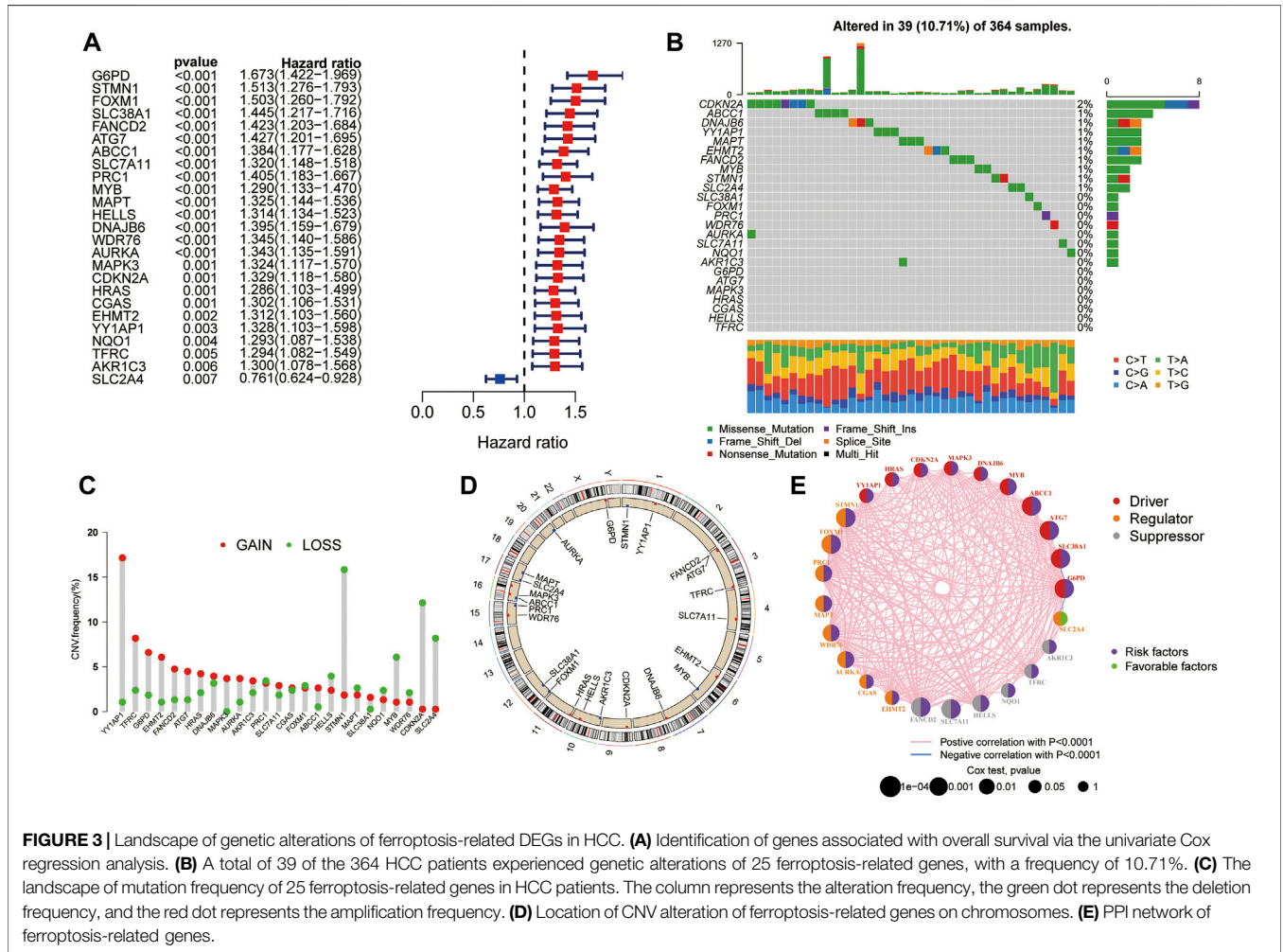


FIGURE 3 | Landscape of genetic alterations of ferroptosis-related DEGs in HCC. **(A)** Identification of genes associated with overall survival via the univariate Cox regression analysis. **(B)** A total of 39 of the 364 HCC patients experienced genetic alterations of 25 ferroptosis-related genes, with a frequency of 10.71%. **(C)** The landscape of mutation frequency of 25 ferroptosis-related genes in HCC patients. The column represents the alteration frequency, the green dot represents the deletion frequency, and the red dot represents the amplification frequency. **(D)** Location of CNV alteration of ferroptosis-related genes on chromosomes. **(E)** PPI network of ferroptosis-related genes.

Immune Cell Infiltrated in Different HCC Clusters

The enrichment scores of immune infiltration levels were calculated by single sample gene set enrichment analysis (ssGSEA). ssGSEA is a popular enrichment algorithm, which was extensively utilized in medical studies (Liu et al., 2021a; Liu et al., 2021b; Liu et al., 2022a; Liu et al., 2022b; Liu et al., 2022c). Data were visualized using multidimensional scaling (MDS) and a Gaussian fitting model. The immune infiltration assessment was performed using the Tumor IMMune Estimation Resource (TIMER; <https://cistrome.shinyapps.io/timer/>) and microenvironment cell population count (MCP-counter) method.

Building a Combined Nomogram for Clinical Practice

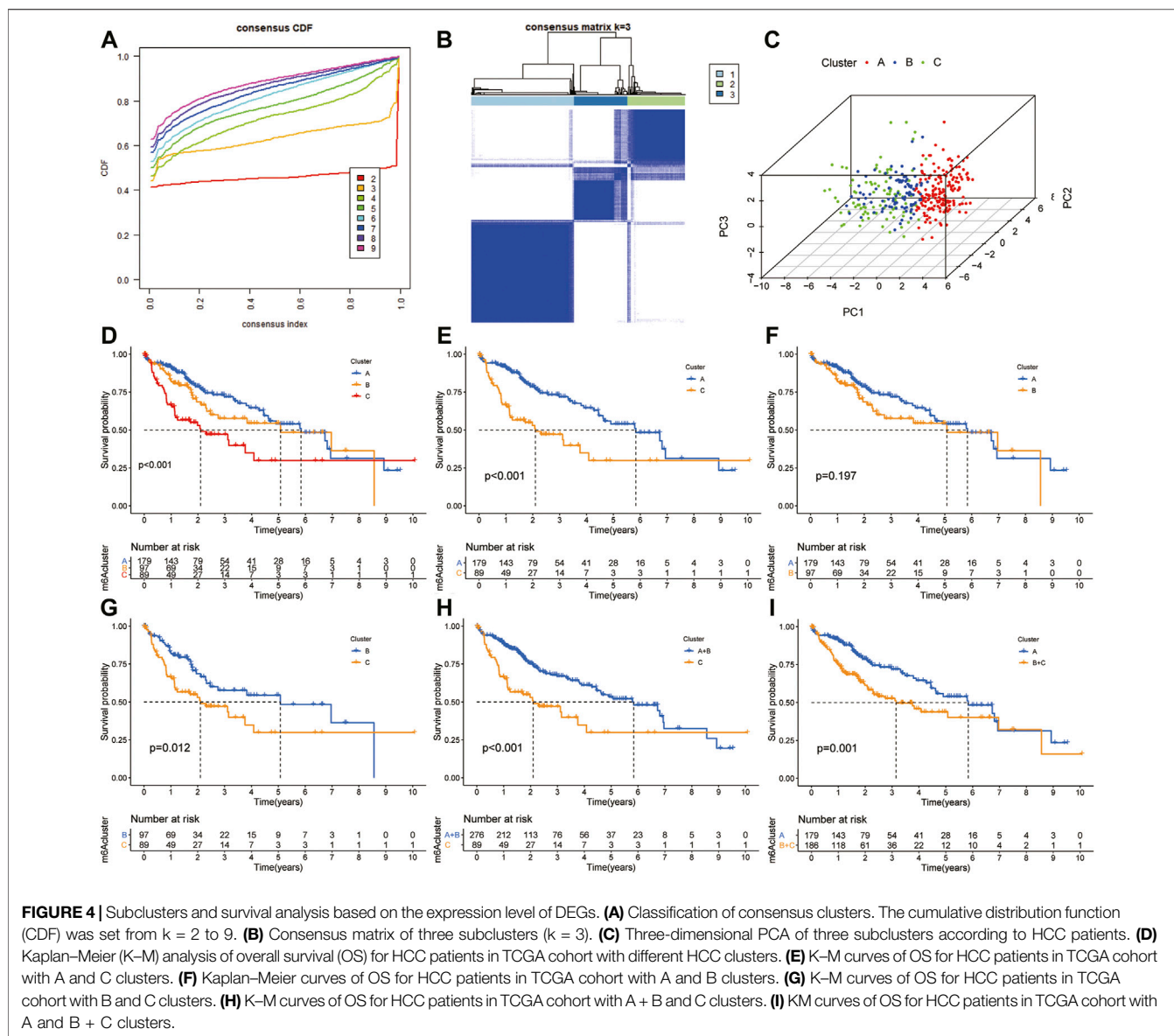
In the present study, a nomogram was constructed based on the risk model and pathological stage to assess the probability of individual patient’s OS with HCC. Meanwhile, the calibration curves were performed to verify the accuracy of the nomogram.

Furthermore, the ROC and DCA were applied to evaluate the prediction efficiency and net benefit of the nomogram for HCC patients at 1, 3, and 5 years.

RESULTS

Identification of Ferroptosis-Related DEGs in Patients With HCC

A workflow of this study is presented in **Figure 1**. Based on the threshold of FDR <0.05 and |log₂ FC| > 1, a total of 51 upregulated and 7 downregulated significant ferroptosis-related differentially expressed genes (DEGs) were identified (**Figure 2A**), and the expression landscape of DEGs was shown in the heatmap (**Figure 2B**). Next, the ferroptosis-related DEGs were selected to perform the GO (**Figure 2C**) and KEGG (**Figure 2D**) analyses. Subsequently, several biological processes, including response to oxidative stress, reactive oxygen species metabolic process, and aging, were detected in GO terms. As to KEGG pathway analysis, ferroptosis, serotonergic synapse, VEGF signaling pathway,



arachidonic acid metabolism, etc. were mostly associated with these genes.

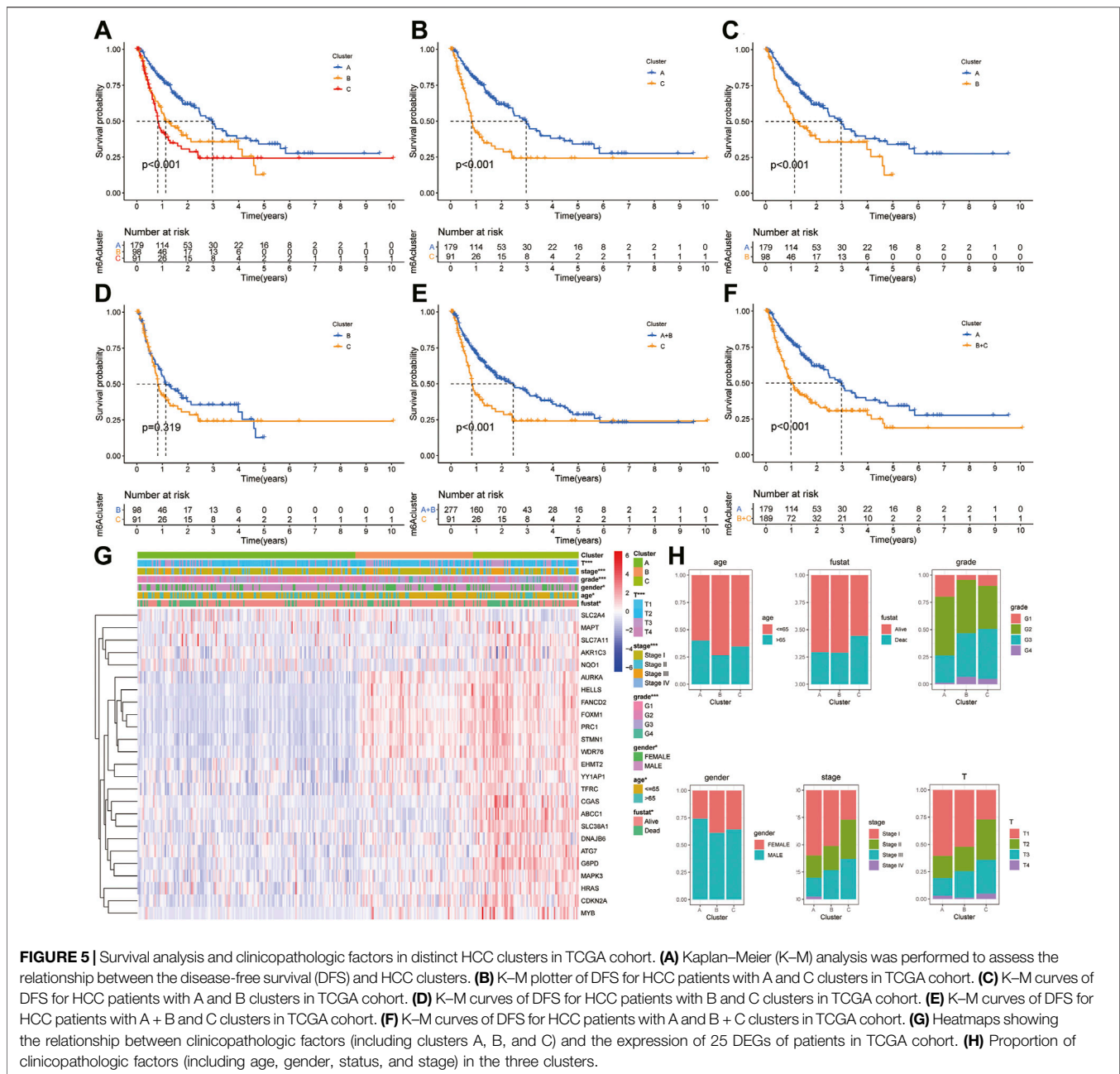
Landscape of Genetic Alterations of Ferroptosis-Related DEGs in HCC

Univariate Cox regression analysis was performed to evaluate the prognostic value of ferroptosis-related DEGs, and 25 DEG aberrant expressions were correlated with the overall survival of HCC patients in TCGA cohort (**Figure 3A**). Mutation analysis of 25 prognostic genes revealed that 10% of genes were mutated by cBioportal (**Figure 3B**). We first figured out the somatic mutation rates of 25 DEGs based on the simple nucleotide variation data from TCGA database. The results revealed that only 39 of the 364 (10.71%) samples presented genetic alterations. We observed CNV changed in YY1AP1, STMN1, CDKN2A, and

SLC2A4 (**Figure 3C**). The location of 25 ferroptosis-related genes on the chromosomes is shown in **Figure 3D**. The PPI network of ferroptosis-related DEGs is constructed in **Figure 3E**.

Consensus Cluster and Survival Analysis

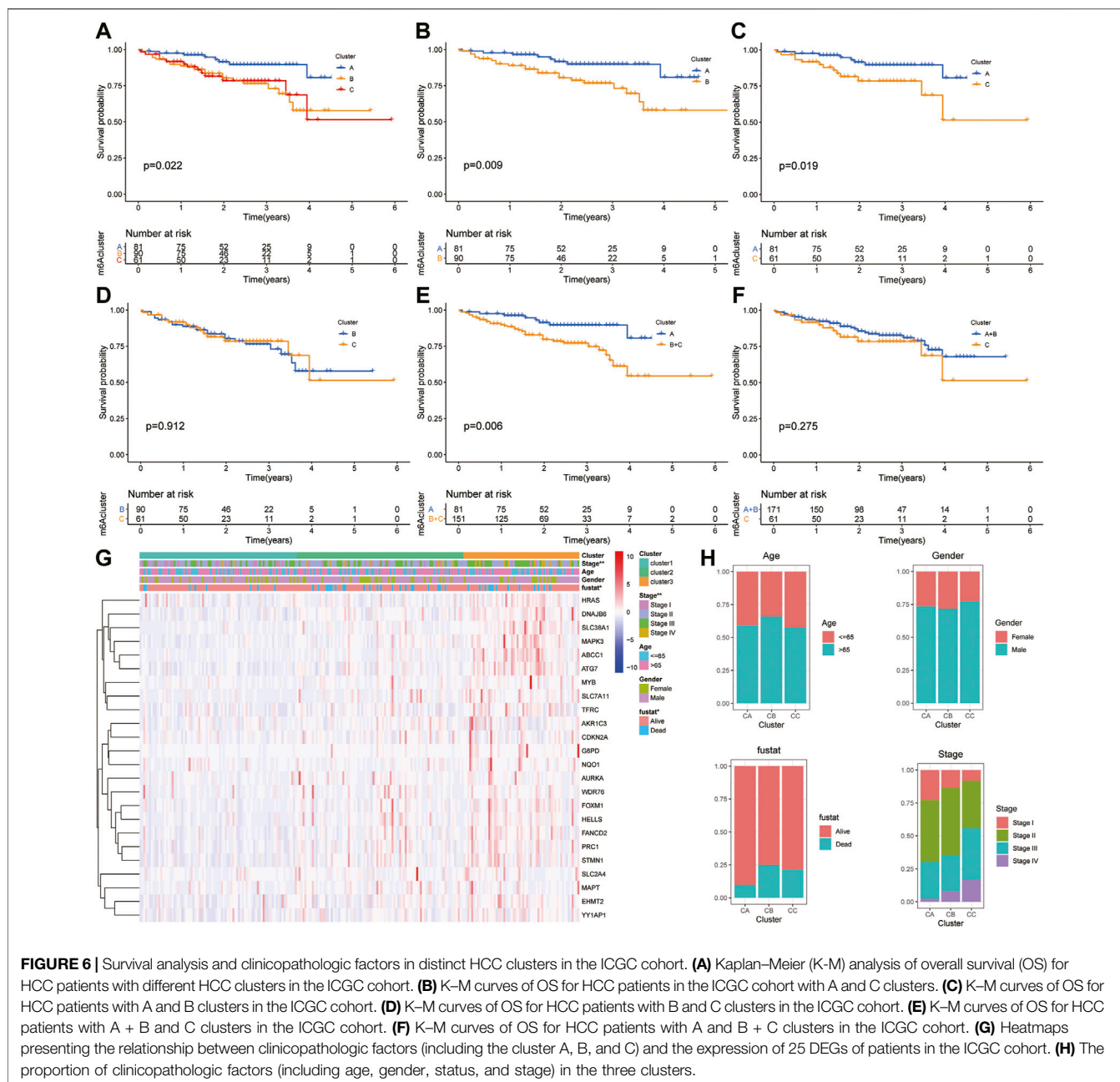
The “ConsensusCluster” package in R language was used to perform consensus clustering analyses of HCC samples from TCGA dataset based on the 25 ferroptosis-related genes shown in **Figures 4A,B**. In order to obtain a reliable and stability cluster, $k = 3$ was chosen from $k = 2$ to 9 in TCGA dataset. However, the PCA analysis revealed that $k = 3$ was also preferable (**Figure 4C**). Then, the HCC patients were split into three distinct clusters: A, B, and C clusters. **Figure 4D** shows an obvious distinction in overall survival among these three clusters. K–M analysis suggested that significant overall survival benefit of the A cluster over B or C cluster, and B cluster over C cluster



(Figures 4D–G). After combining clusters A and B, a significantly longer overall survival was shown for A + B than for C by log-rank tests ($p < 0.001$; Figure 4H). In addition, after combining clusters B and C, a significantly longer overall survival was shown for A than for B + C by log-rank tests ($p < 0.001$; Figure 4I). A clear disease-free survival (DFS) difference among the three clusters was observed ($p < 0.001$; Figure 5A). The DFS was longer for cluster A than for cluster B patients, and cluster B patients than for cluster C patients. The DFS in cluster A was significantly longer than that in clusters B and C ($p < 0.001$, respectively; Figure 5B,C). The DFS was longer for cluster B than for cluster C patients ($p < 0.001$; Figure 5D). After combining clusters A and B, a significantly longer overall survival was shown

for A + B than for C by log-rank tests ($p < 0.001$; Figure 5E). In addition, after combining clusters B and C, a significantly longer overall survival was shown for A than for B + C by log-rank tests ($p < 0.001$; Figure 5F). Figures 5G,H indicate that the three clusters had different clinicopathologic features, including T stage, tumor stage, grade, gender, age, and survival status.

Moreover, the ICGC cohort was regarded as the external validation set. Figure 6A shows an obvious distinction in overall survival among these three clusters ($p = 0.022$). Figures 6B,C show patients in cluster A had longer OS time than patients in cluster B ($p = 0.009$) and cluster C ($p = 0.019$). But the survival difference between clusters B and C was not significant ($p = 0.912$) (Figure 6D). After combining clusters

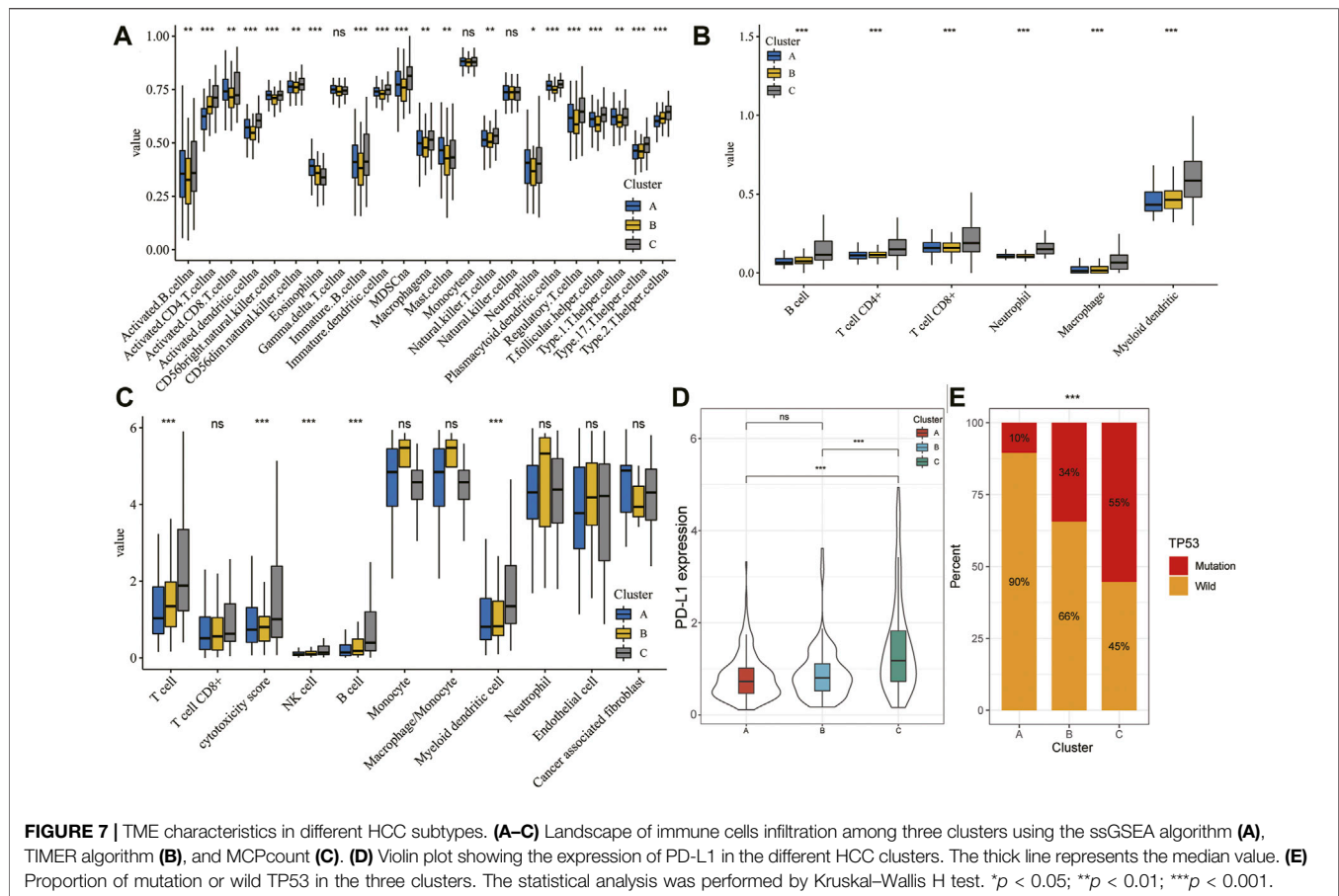


B and C, patients in cluster A presented longer OS time than patients in clusters B + C (**Figure 6E**; $p = 0.006$). But the survival difference between clusters A + B and C was not significant (**Figure 6F**; $p = 0.275$). The analysis further showed there were significant differences in the TNM stage and survival status (**Figures 6G,H**).

Immunoinflammatory Cells Infiltrating in Different Ferroptosis-Related Clusters

Immune cells are well known to be the key part for antitumor immune response and immunotherapy; therefore, we examined the distribution of immune cell infiltration in the three clusters

based on the ssGSEA algorithm (**Figure 7A**). A higher ssGSEA score indicated more infiltrating immune cells. The results showed that activated CD4+/CD8+ T cells, effector memory CD4+/CD8+ T cells, activated dendritic cells, activated B cells, immature B cells, immature dendritic cells, MDSC, regulatory T cells, T follicular helper cells, and type 17 T helper cells were mainly enriched in the C subtype. However, eosinophils were markedly enriched in the A subtype. Furthermore, we also assessed the immune infiltration level using TIMER and MCPcount algorithms, which indicated a significant difference between the three clusters (**Figures 7B,C**; $p < 0.05$). In addition, there was clear difference in the expression of PD-L1 and TP53 between the three clusters (**Figures 7D,E**; $p < 0.05$).



Pathway Enrichment Analysis of Different Ferroptosis-Related Clusters

To explore the biological molecular changes among these ferroptosis-related clusters, we performed GSEA enrichment. Heatmap showed that P53 pathway, DNA replication, and cell cycle were more enriched in cluster B than in cluster A (**Figure 8A**); cell cycle, DNA replication, and mismatch repair were more enriched in cluster C than in cluster A (**Figure 8B**); the and PPAR pathway, fatty acid metabolism, and multiple metabolism pathway were more enriched in cluster C than in cluster B (**Figure 8C**). The color changes from yellow to red, determining an increase in the value of the enriched score. Blue represents cluster A, yellow represents cluster B, and red represents cluster C. GSEA showed that multiple metabolic and cell cycle pathways were identified. A total of 1,966 differential genes were obtained among the three clusters (**Figure 8D**). Functional enrichment analysis was performed through the GO and KEGG (**Figures 8E,F**).

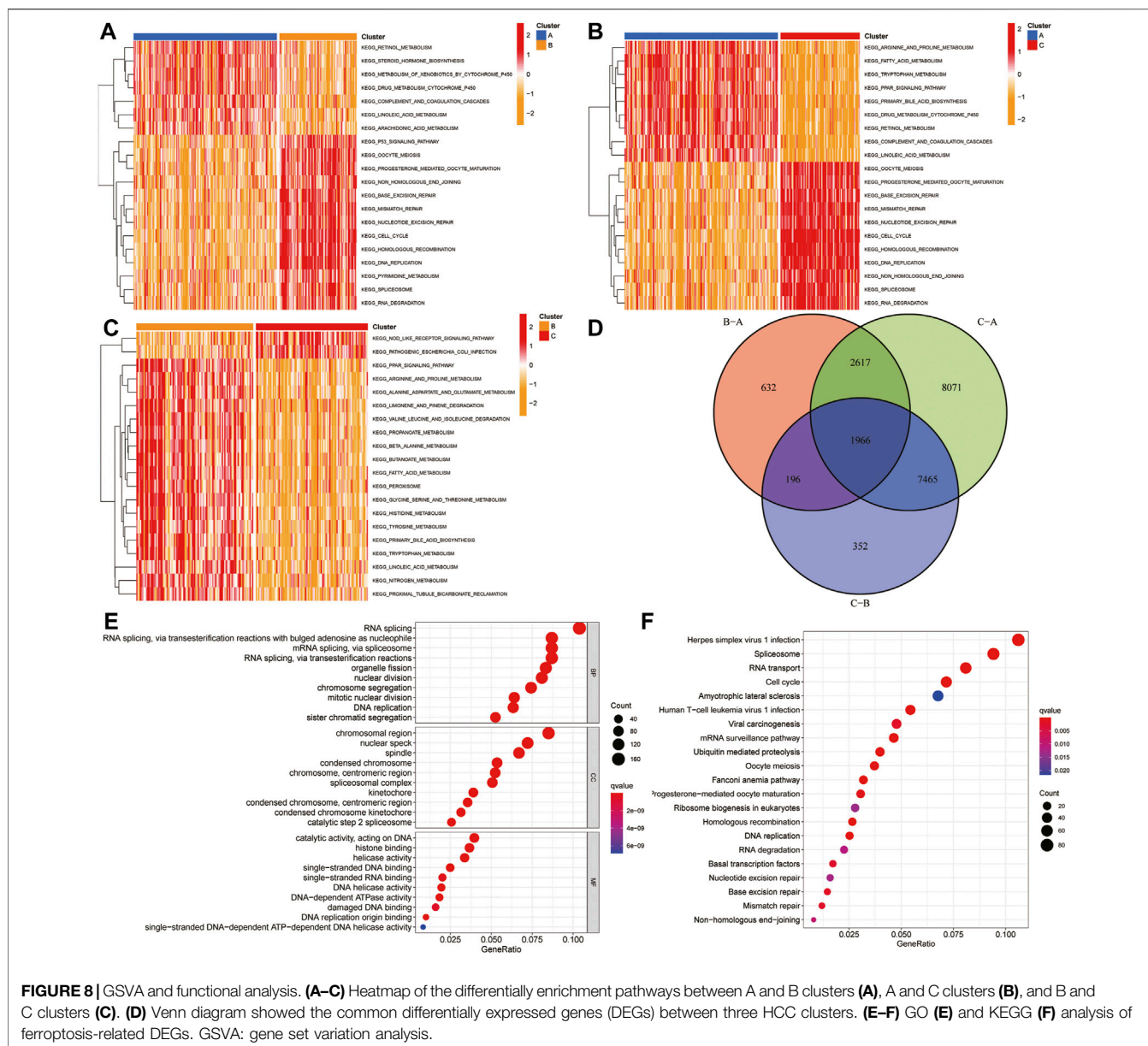
Development of an Integrated Signature

Based on the univariate Cox regression analysis of TCGA cohort, genes with significant prognostic value were further extracted ($p < 0.01$; **Figure 9A**). By the random survival forest variable hunting (RSFVH) algorithm, the top 10 genes were ranked based on their predictive importance: TMEM251, MED8, UCK2, STIP1, FIGU,

PPM1G, ZDHHC18, MUTYH, RAN, and SNRPB (**Figure 9B**). We performed Kaplan–Meier analysis to figure out the best risk model with relatively small genes and relative significant p value. Then, we found the five-gene signature ranked top, including MED8, FIGU, PPM1G, RAN, and SNRPB (**Figure 9C**). Subsequently, we inspected the distribution of risk score and survival status in high- and low-risk groups, and the results demonstrated that the high-risk group presented a higher risk score and rates of death than the low-risk group (**Figure 9D**). The heatmap showed that the five gene had a higher expression level in the high-risk group than the low-risk group (**Figure 9D**). Similar results were found in the ICGC cohort (**Figure 9E**).

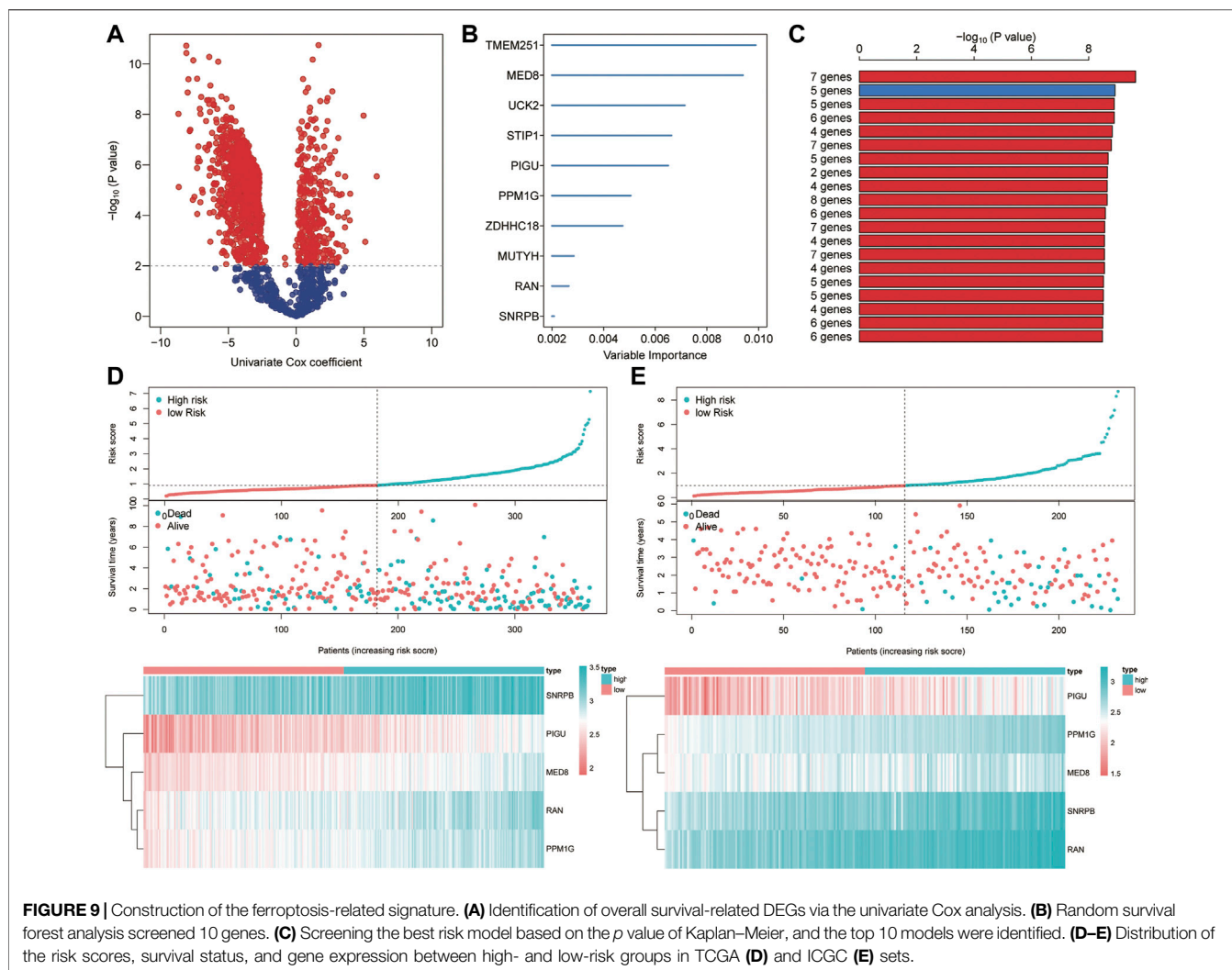
Kaplan–Meier and Time-dependent ROC Curves of Five-Gene Signature

The HCC patients were split into high-risk and low-risk groups by the median risk score. In the training set, K–M analysis indicated that the patients with high-risk scores had worse overall survival than patients with low-risk scores (HR = 2.52, 95% CI:1.78–3.57, log-rank test $p < 0.001$) (**Figure 10A**). In the ICGC dataset, the overall survival of patients with low-risk scores was significantly longer than that of patients with high-risk scores (HR = 7.45, 95% CI: 4.09–13.59, log-rank test $p < 0.001$) (**Figure 10B**). To further understand the predictive ability at 0.5, 1, 2, 3, and 5 years of the



signature, we used time–ROC analysis in TCGA (**Figure 10C**) and ICGC (**Figure 10D**) cohorts. The AUC of the signature in TCGA cohort was 0.764, 0.768, 0.712, 0.722, and 0.702 at 0.5, 1, 2, 3, and 5 years, respectively (**Figure 9C**). The AUC in the ICGC cohort was 0.725, 0.746, 0.801, and 0.823, 0.785 at 0.5, 1, 2, 3, and 5 years (**Figure 10D**). These suggest that the risk model provided a reliable predictive efficiency in HCC prognosis. Univariate Cox analysis was performed on all factors, and multivariate Cox analysis was performed with variates which had $p < 0.05$ of the univariate Cox analyses in TCGA (**Figure 10E**) and ICGC (**Figure 10F**) cohorts. The results confirmed that the clinical stage and risk score were stronger independent poor prognostic factors in both cohorts. To further determine the robustness of the risk mode, we performed an additional analysis to predict the overall survival of HCC patients in an independent GEO cohort (GSE14520). Similarly,

K–M curves showed that the patient with high-risk had worse overall survival (**Supplementary Figure S1A**). The AUC of the signature was 0.73, 0.671, 0.610, 0.581, and 0.606 at 0.5, 1, 2, 3, and 5 years, respectively (**Supplementary Figure S1B**). The univariate and multivariate Cox regression analyses demonstrated that the risk score was an independent risk factor for the overall survival of HCC (**Supplementary Figure S1C**). This result was validated by another independent cohort CPTAC in the protein level, which completely echoed the result that high-risk patients appeared to present a poorer overall survival than those with low-risk scores. The AUC of the signature in the CPTAC cohort is 0.606 at 0.5 year, 0.706 at 1 year, 0.662 at 2 years, 0.672 at 3 years, and 0.702 at 5 years. Univariate and multivariate Cox analyses also demonstrated that protein risk score was an independent prognostic indicator in the protein level.



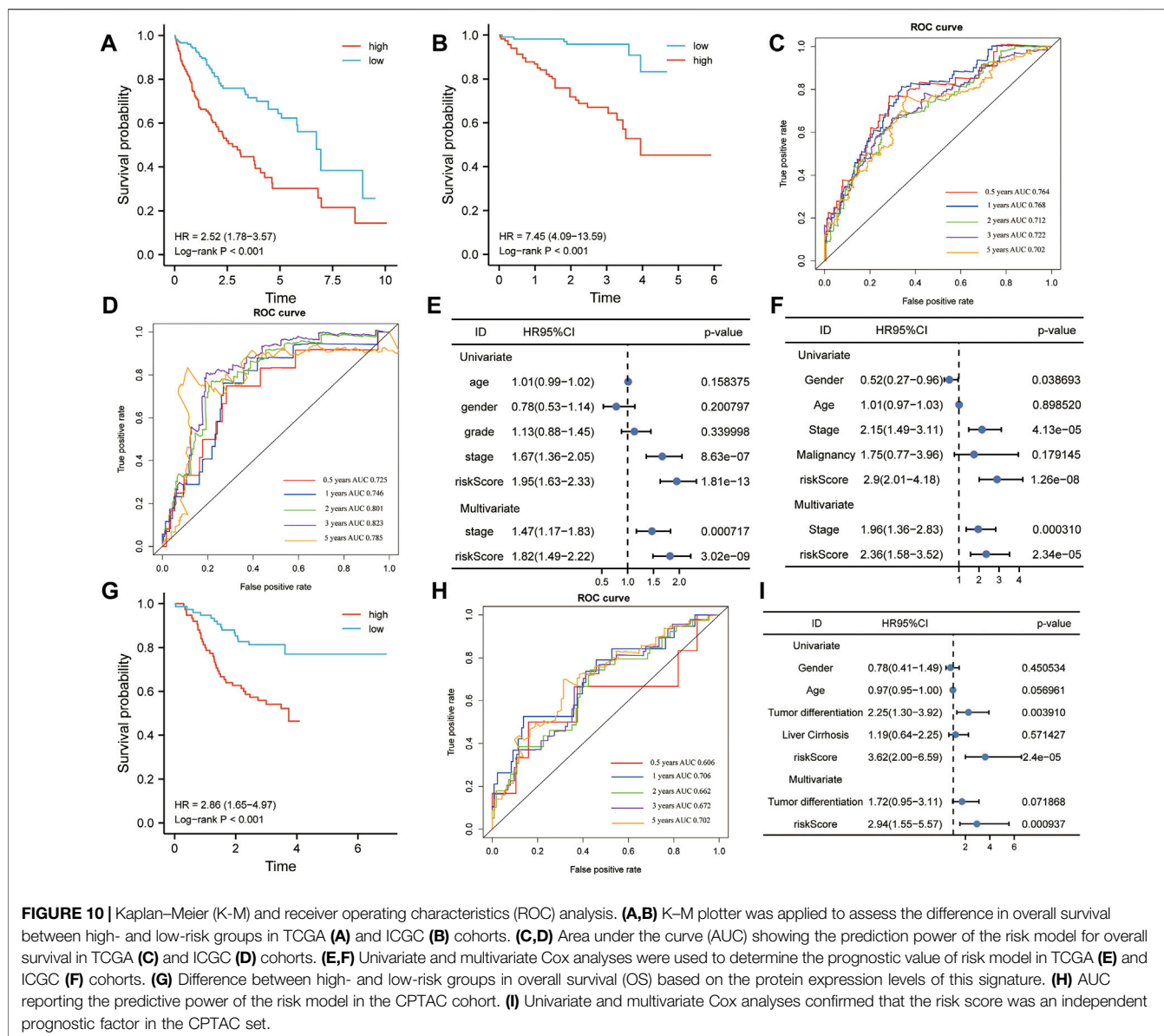
The Relationship Between the Risk Score and Clinical Pathological

Considering the complexity of the relationship between ferroptosis and HCC, we illustrated the workflow of risk score construction with the alluvial diagram (Figure 11A). These results indicated that cluster A was linked to a lower risk score, whereas B and C clusters exhibited higher risk scores (Figure 11A). We also explored the relationship between the risk score and HCC subtype and found that the A subtype was associated with the lowest risk score, and C subtype was associated with the highest risk score (Figure 11B). The relationship between the risk score and alive or dead status showed that the patients with dead status were associated with a higher risk score than those with alive status (Figure 11C). The relationship between the risk score and difference grades showed that the patients with a higher grade appeared to be associated with a higher risk score (Figure 11D). The relationship between the risk score and difference in tumor stages showed that the patients with higher difference in tumor stages appeared to be associated with a higher risk score (Figure 11E). The relationship between the risk score and difference TNM stages showed that the patients with

higher difference in TNM stage appeared to be associated with a higher risk score (Figure 11F). The alive patients were confirmed with low-risk score than those with high-risk score (alive vs dead: 77 vs 23% in the low-risk score group and 56 vs 44% in the high-risk score group; Figure 11G). The lower grade was confirmed in patients with low-risk score compared to those with high-risk score (G1 vs G2 vs G3 vs G4: 16 vs 55% vs 27 vs 2% in the low-risk score group, 11 vs 43% vs 41 vs 5% in the high-risk score group; Figure 11H). A consistent result was also observed in the tumor stage (Figure 11I) and TNM stage (Figure 11J). Collectively, these results revealed that the risk score is related to the tumor stage and correlates with the prognosis of HCC patients.

Building a Combined Nomogram for Clinical Practice

We built a comprehensive nomogram that could be applied in clinical practice based on the risk score and clinical stage (Figure 12A). Then, the calibration curves were performed to assess the prediction value of this nomogram (Figure 12B). The



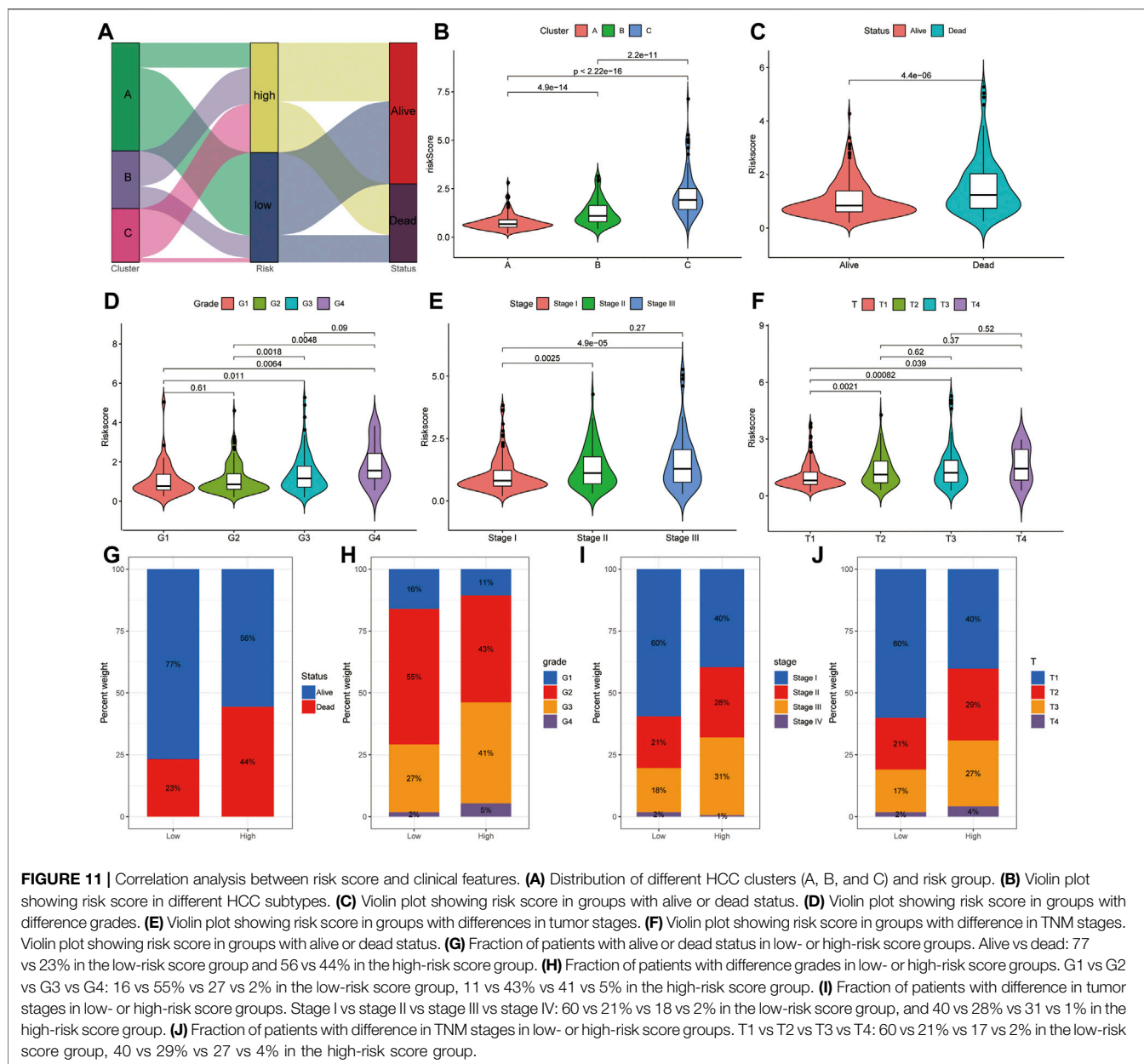
results demonstrated that the calibration curve for stage and risk score agreed well with the ideal observations. Furthermore, ROC analysis revealed that the combined nomogram showed the best performances in predicting the overall survival of HCC patients, compared to the risk score and clinical stage (AUC = 0.77 at 1 year, 0.76 at 3 years, and 0.74 at 5 years, **Figure 12C**). In addition, decision curve analysis indicated that the combined model achieved greater net benefit than the stage or risk score alone (**Figure 12D**).

DISCUSSION

The number of HCC patients and the mortality rates still show a growing trend globally (Couri and Pillai, 2019). Sorafenib resistance remains a big challenge in the short-term treatment and long-term prognosis of patients with HCC. Mounting evidence has shown that

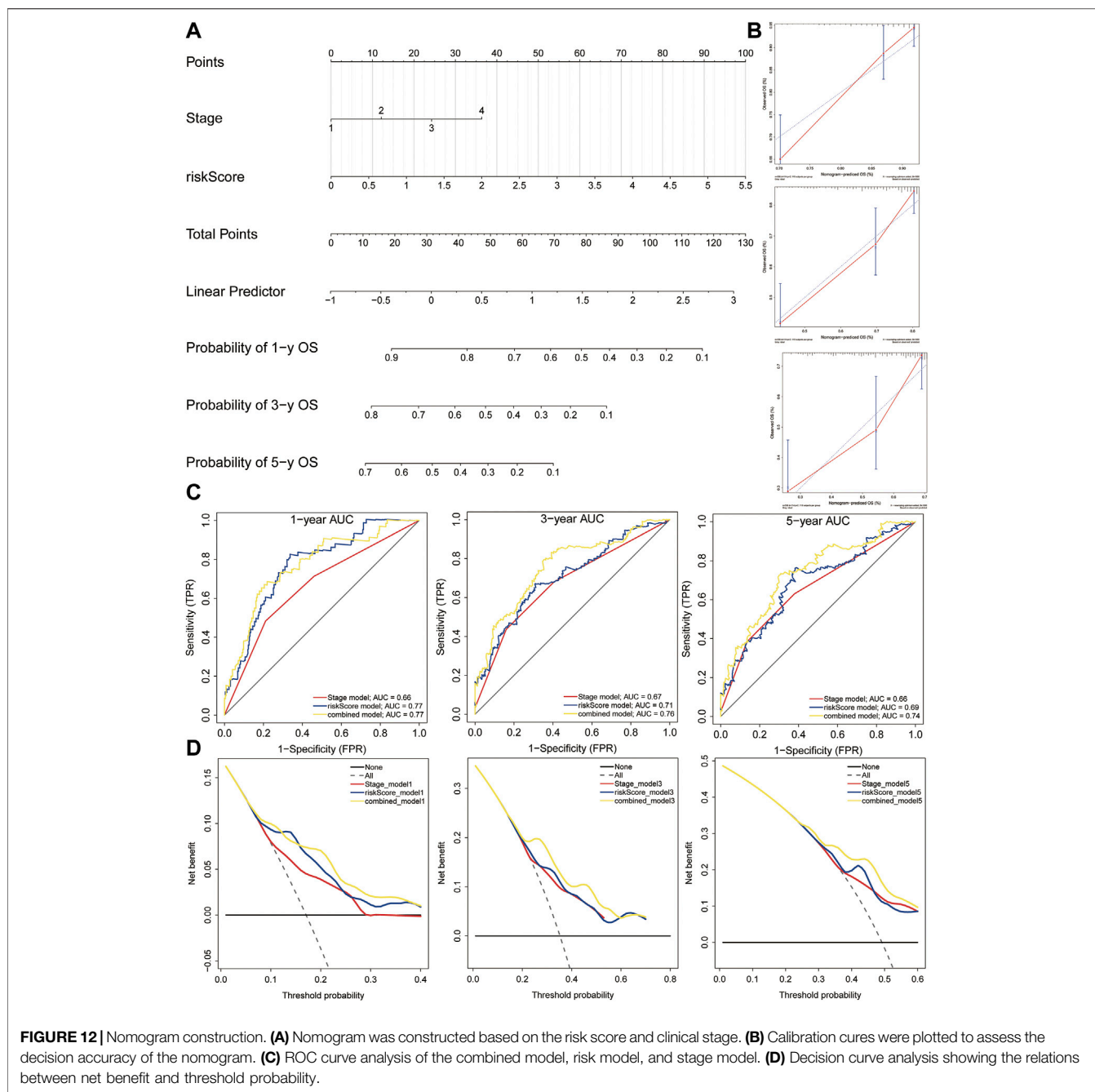
ferroptosis-related genes play an essential role in sorafenib resistance (Nie et al., 2018; Viveiros et al., 2019) and anticancer immunity (Angeli et al., 2019). Herein, this study analyzed 752 HCC patients and found a good indicator for prognosis prediction guidance, which is named a combined nomogram. The nomogram could predict the survival of patients with HCC.

In recent years, accumulating studies have reported several ferroptosis-related gene models in the pathogenesis of HCC. Kai Wen et al. obtained the ferroptosis-related genes from the FerrFb database and constructed a 10-gene signature via univariate and LASSO Cox regression (Wen et al., 2021). Hao Zhang et al. obtained the ferroptosis-related genes from the KEGG pathway and GSEA databases and built a 7-gene signature based on the univariate and LASSO Cox regression (Zhang et al., 2021). Jie-ying Liang et al. acquired 60 ferroptosis-related genes from the previous studies and constructed a 10-gene signature using the univariate and LASSO



Cox regression (Liang et al., 2020). Lijun Xu et al. retrieved 173 ferroptosis-related genes and 120 pyroptosis-related genes from the FerrDb and GeneCards website and constructed a 13-gene signature through univariate and LASSO Cox regression (Xu et al., 2022). Jukun Wang et al. acquired 60 ferroptosis-related genes from the previous studies and constructed a 3-gene signature using the univariate and LASSO Cox regression (Wang J. et al., 2021). Tuo Deng et al. obtained 41 ferroptosis-related genes from the KEGG database and identified 8 genes associated with the methylation status and overall survival of HCC. Subsequently, the unsupervised consensus clustering was performed and established a 15-gene signature based on the differentially expressed genes between ferroptosis-H and ferroptosis-L groups via the univariate and LASSO Cox regression (Deng et al., 2021). There are many

possibilities to extending the ferroptosis-related gene model. In the present study, 287 ferroptosis-related genes were retrieved from the FerrDb database and previous studies. Subsequently, a total of 58 ferroptosis-related DEGs were identified in TCGA cohort, and 25 DEGs were further confirmed to be significantly associated with the prognostic of HCC patients. Next, we conducted consensus clustering analyses of HCC samples from TCGA dataset based on the 25 ferroptosis-related genes. Subsequently, the overall and disease-free survival rates were examined in detail among three clusters using Kaplan–Meier curves in TCGA cohort. These results were further validated in the ICGC cohort. Taking immune infiltration into consideration will help us understand the role of ferroptosis-related genes. The A cluster was characterized by eosinophilia, the C cluster was characterized by effector memory



CD4+/CD8+ T cells, activated CD4+/CD8+ T cells, activated B cells, activated dendritic cells, immature B cells, immature dendritic cells, MDSC, regulatory T cells, T follicular helper cells, and type 17 T helper cells. The three distinct HCC clusters were associated with the infiltration of immunoinflammatory cells and the expression of PD-L1 and TP53 mutation. Then, by the univariate Cox regression and random survival forest variable hunting (RSFVH) algorithm, the top 10 genes were ranked based on their predictive importance. Furthermore, because 10 genes could form a total of $2^{10-1} = 1,023$ risk models, we performed Kaplan–Meier analysis to figure out the best risk model with relatively small genes and relatively significant

p value. Hence, this is clearly different from other prediction models, including the LASSO risk model. Finally, a 5-gene signature was constructed and externally validated in several external datasets, including MED8, FIGU, PPM1G, RAN, and SNRPB. Furthermore, this result was validated by another independent cohort CPTAC in the protein level. According to the value of hazard ratio (HR), they were considered as the risk genes. Mediator complex subunit 8 (MED8) correlated with poorer overall survival and advanced clinical stage and showed higher expression in metastatic than primary tumors in clear cell RCC (Syng et al., 2016). Phosphatidylinositol glycan anchor biosynthesis class U

(PIGU) may promote HCC progression by activating the NF- κ B pathway (Wei et al., 2020) and could be an oncogene in HCC (Cao et al., 2019). PPM1G, protein phosphatase, Mg²⁺/Mn²⁺-dependent 1G, was reported to promote the progression of HCC by regulating the alternative splicing of SRSF3 (Chen et al., 2021). RAN, a member of RAS oncogene family, could promote the proliferation and migration ability of head and neck squamous cell carcinoma cells (Zhang et al., 2020). SNRPB, small nuclear ribonucleoprotein polypeptides B and B1, has been reported to promote HCC progression by inducing metabolic reprogramming (Chen et al., 2020). In general, these five genes in the signature were all cancer-promoting genes. While the effectiveness of a single clinical factor is insufficient, a multiple-factor signature may bring about changes in personalized HCC treatment. Consequently, a ferroptosis-related signature was constructed in the training group by univariate Cox regression, RSFVH algorithm, and Kaplan–Meier analyses. To make it suitable for the application in clinical HCC diagnosis, a nomogram was constructed to make better individualized treatment. This proposed model is one of the more realistic models than earlier models reported in the literature. We performed unsupervised cluster analysis based on 25 survival-related genes and examined in greater detail the differences in prognostic, immune cell infiltration, PD-L1 expression, and TP53 mutations among three subclusters. We collected more comprehensive resource of ferroptosis-related genes and constructed a more robust risk model using multiple machine learning methods.

Nevertheless, several limitations still remain in the present study. In this study, we only explored the correlation between ferroptosis-related genes and immune cell infiltration and PD-L1 and TP53 mutations and did not explain the role and underlying mechanisms of ferroptosis in the immune response of HCC. Therefore, further *in vivo* and *in vitro* experiments are necessary to validate these mechanisms.

REFERENCES

- Angeli, J. P. F., Krysko, D. V., and Conrad, M. (2019). Ferroptosis at the Crossroads of Cancer-Acquired Drug Resistance and Immune Evasion. *Nat. Rev. Cancer* 19, 405–414. doi:10.1038/s41568-019-0149-1
- Cao, J., Wang, P., Chen, J., and He, X. (2019). PIGU Overexpression Adds Value to TNM Staging in the Prognostic Stratification of Patients with Hepatocellular Carcinoma. *Hum. Pathol.* 83, 90–99. doi:10.1016/j.humpath.2018.08.013
- Capelletti, M. M., Manceau, H., Puy, H., and Peoc'h, K. (2020). Ferroptosis in Liver Diseases: An Overview. *Ijms* 21, 4908. doi:10.3390/ijms21144908
- Chen, D., Zhao, Z., Chen, L., Li, Q., Zou, J., and Liu, S. (2021). PPM1G Promotes the Progression of Hepatocellular Carcinoma via Phosphorylation Regulation of Alternative Splicing Protein SRSF3. *Cell Death Dis* 12, 722. doi:10.1038/s41419-021-04013-y
- Chen, W., Ma, T., Zhang, J., Zhang, X., Chen, W., Shen, Y., et al. (2020). A Systematic Review and Meta-Analysis of Adjuvant Transarterial Chemoembolization after Curative Resection for Patients with Hepatocellular Carcinoma. *Hpb* 22, 795–808. doi:10.1016/j.hpb.2019.12.013
- Couri, T., and Pillai, A. (2019). Goals and Targets for Personalized Therapy for HCC. *Hepatol. Int.* 13, 125–137. doi:10.1007/s12072-018-9919-1
- Deng, T., Hu, B., Jin, C., Tong, Y., Zhao, J., Shi, Z., et al. (2021). A Novel Ferroptosis Phenotype-Related Clinical-molecular Prognostic Signature for Hepatocellular Carcinoma. *J. Cel Mol Med* 25, 6618–6633. doi:10.1111/jcmm.16666
- Gorgen, A., Galvin, Z., Huang, A. C., Vinaixa, C., O'Rourke, J. M., Francoz, C., et al. (2020). The Impact of Direct-Acting Antivirals on Overall Mortality and Tumoral Recurrence in Patients with Hepatocellular Carcinoma Listed for Liver Transplantation: An International Multicenter Study. *Transplantation* 104, 2087–2096. doi:10.1097/TP.0000000000003115
- Hänzelmann, S., Castelo, R., and Guinney, J. (2013). GSVA: Gene Set Variation Analysis for Microarray and RNA-Seq Data. *BMC Bioinformatics* 14, 7. doi:10.1186/1471-2105-14-7
- Hilmi, M., Neuzillet, C., Calderaro, J., Lafdil, F., Pawlowsky, J.-M., and Rousseau, B. (2019). Angiogenesis and Immune Checkpoint Inhibitors as Therapies for Hepatocellular Carcinoma: Current Knowledge and Future Research Directions. *J. Immunotherapy Cancer* 7, 333. doi:10.1186/s40425-019-0824-5
- Kudo, M., Finn, R. S., Qin, S., Han, K.-H., Ikeda, K., Piscaglia, F., et al. (2018). Lenvatinib versus Sorafenib in First-Line Treatment of Patients with Unresectable Hepatocellular Carcinoma: a Randomised Phase 3 Non-inferiority Trial. *The Lancet* 391, 1163–1173. doi:10.1016/S0140-6736(18)30207-1
- Kulik, L., and El-Serag, H. B. (2019). Epidemiology and Management of Hepatocellular Carcinoma. *Gastroenterology* 156, 477–491. doi:10.1053/j.gastro.2018.08.065
- Li, J., Cao, F., Yin, H.-l., Huang, Z.-j., Lin, Z.-t., Mao, N., et al. (2020). Ferroptosis: Past, Present and Future. *Cel Death Dis* 11, 88. doi:10.1038/s41419-020-2298-2
- Liang, J.-y., Wang, D.-s., Lin, H.-c., Chen, X.-x., Yang, H., Zheng, Y., et al. (2020). A Novel Ferroptosis-Related Gene Signature for Overall Survival Prediction in Patients with Hepatocellular Carcinoma. *Int. J. Biol. Sci.* 16, 2430–2441. doi:10.7150/ijbs.45050

In summary, our study demonstrated that a five-gene signature, and a combined nomogram can predict individual survival of patients with HCC. This study highlights the promising potential of the novel signature, the nomogram can function as the prognostic indicators for individual survival prediction and therapeutic decision-making.

DATA AVAILABILITY STATEMENT

The original contributions presented in the study are included in the article/**Supplementary Material**, further inquiries can be directed to the corresponding authors.

AUTHOR CONTRIBUTIONS

WL, LG, and HZ designed the study. WL, JL, LG, DZ, and HZ participated in drafting the manuscript. WL, JL, and DZ contributed to constructing all figures. All authors read and approved the final manuscript.

FUNDING

This work was supported by the Undergraduate Research Training Program (UGRTP) (Grant No. LE0003).

SUPPLEMENTARY MATERIAL

The Supplementary Material for this article can be found online at: <https://www.frontiersin.org/articles/10.3389/fgene.2022.844624/full#supplementary-material>.

- Liu, Z., Guo, C., Dang, Q., Wang, L., Liu, L., Weng, S., et al. (2022a). Integrative Analysis from Multi-center Studies Identifies a Consensus Machine Learning-Derived lncRNA Signature for Stage II/III Colorectal Cancer. *EBioMedicine* 75, 103750. doi:10.1016/j.ebiom.2021.103750
- Liu, Z., Guo, C., Li, J., Xu, H., Lu, T., Wang, L., et al. (2021a). Somatic Mutations in Homologous Recombination Pathway Predict Favourable Prognosis after Immunotherapy across Multiple Cancer Types. *Clin. Translational Med* 11, e619. doi:10.1002/ctm.2619
- Liu, Z., Liu, L., Guo, C., Yu, S., Meng, L., Zhou, X., et al. (2021b). Tumor Suppressor Gene Mutations Correlate with Prognosis and Immunotherapy Benefit in Hepatocellular Carcinoma. *Int. Immunopharmacology* 101, 108340. doi:10.1016/j.intimp.2021.108340
- Liu, Z., Liu, L., Weng, S., Guo, C., Dang, Q., Xu, H., et al. (2022b). Machine Learning-Based Integration Develops an Immune-Derived lncRNA Signature for Improving Outcomes in Colorectal Cancer. *Nat. Commun.* 13, 816. doi:10.1038/s41467-022-28421-6
- Liu, Z., Wang, Q., Wang, X., Xu, Z., Wei, X., and Li, J. (2020). Circular RNA ciARS Regulates Ferroptosis in HCC Cells through Interacting with RNA Binding Protein ALKBH5. *Cell Death Discov.* 6, 72. doi:10.1038/s41420-020-00306-x
- Liu, Z., Xu, H., Weng, S., Ren, Y., and Han, X. (2022c). Stemness Refines the Classification of Colorectal Cancer with Stratified Prognosis, Multi-Omics Landscape, Potential Mechanisms, and Treatment Options. *Front. Immunol.* 13, 828330. doi:10.3389/fimmu.2022.828330
- Llovet, J. M., Ricci, S., Mazzaferro, V., Hilgard, P., Gane, E., Blanc, J.-F., et al. (2008). Sorafenib in Advanced Hepatocellular Carcinoma. *N. Engl. J. Med.* 359, 378–390. doi:10.1056/NEJMoa0708857
- Louandre, C., Ezzoukry, Z., Godin, C., Barbare, J.-C., Mazière, J.-C., Chauffert, B., et al. (2013). Iron-dependent Cell Death of Hepatocellular Carcinoma Cells Exposed to Sorafenib. *Int. J. Cancer* 133, 1732–1742. doi:10.1002/ijc.28159
- Nie, J., Lin, B., Zhou, M., Wu, L., and Zheng, T. (2018). Role of Ferroptosis in Hepatocellular Carcinoma. *J. Cancer Res. Clin. Oncol.* 144, 2329–2337. doi:10.1007/s00432-018-2740-3
- Ritchie, M. E., Phipson, B., Wu, D., Hu, Y., Law, C. W., Shi, W., et al. (2015). Limma powers Differential Expression Analyses for RNA-Sequencing and Microarray Studies. *Nucleic Acids Res.* 43, e47. doi:10.1093/nar/gkv007
- Subramanian, A., Tamayo, P., Mootha, V. K., Mukherjee, S., Ebert, B. L., Gillette, M. A., et al. (2005). Gene Set Enrichment Analysis: a Knowledge-Based Approach for Interpreting Genome-wide Expression Profiles. *Proc. Natl. Acad. Sci. U.S.A.* 102, 15545–15550. doi:10.1073/pnas.0506580102
- Sun, X., Ou, Z., Chen, R., Niu, X., Chen, D., Kang, R., et al. (2016). Activation of the P62-Keap1-NRF2 Pathway Protects against Ferroptosis in Hepatocellular Carcinoma Cells. *Hepatology* 63, 173–184. doi:10.1002/hep.28251
- Syring, I., Klümper, N., Offermann, A., Braun, M., Deng, M., Boehm, D., et al. (2016). Comprehensive Analysis of the Transcriptional Profile of the Mediator Complex across Human Cancer Types. *Oncotarget* 7, 23043–23055. doi:10.18632/oncotarget.8469
- Tabrizian, P., Jibara, G., Shrager, B., Schwartz, M., and Roayaie, S. (2015). Recurrence of Hepatocellular Cancer after Resection. *Ann. Surg.* 261, 947–955. doi:10.1097/SLA.0000000000000710
- Viveiros, P., Riaz, A., Lewandowski, R. J., and Mahalingam, D. (2019). Current State of Liver-Directed Therapies and Combinatory Approaches with Systemic Therapy in Hepatocellular Carcinoma (HCC). *Cancers* 11, 1085. doi:10.3390/cancers11081085
- Wang, J., Han, K., Zhang, C., Chen, X., Li, Y., Zhu, L., et al. (2021). Identification and Validation of Ferroptosis-Associated Gene-Based on Immune Score as Prognosis Markers for Hepatocellular Carcinoma Patients. *J. Gastrointest. Oncol.* 12, 2345–2360. doi:10.21037/jgo-21-237
- Wang, Q., Bin, C., Xue, Q., Gao, Q., Huang, A., Wang, K., et al. (2021). GSTZ1 Sensitizes Hepatocellular Carcinoma Cells to Sorafenib-Induced Ferroptosis via Inhibition of NRF2/GPX4 axis. *Cel Death Dis* 12, 426. doi:10.1038/s41419-021-03718-4
- Wei, X., Yang, W., Zhang, F., Cheng, F., Rao, J., and Lu, L. (2020). PIGU Promotes Hepatocellular Carcinoma Progression through Activating NF-Kb Pathway and Increasing Immune Escape. *Life Sci.* 260, 118476. doi:10.1016/j.lfs.2020.118476
- Wen, K., Yan, Y., Shi, J., Hu, L., Wang, W., Liao, H., et al. (2021). Construction and Validation of a Combined Ferroptosis and Hypoxia Prognostic Signature for Hepatocellular Carcinoma. *Front. Mol. Biosci.* 8, 809672. doi:10.3389/fmolb.2021.809672
- Wilkerson, M. D., and Hayes, D. N. (2010). ConsensusClusterPlus: a Class Discovery Tool with Confidence Assessments and Item Tracking. *Bioinformatics* 26, 1572–1573. doi:10.1093/bioinformatics/btq170
- Xu, L., Zheng, Q., and Liu, W. (2022). Combination of Ferroptosis and Pyroptosis to Construct a Prognostic Classifier and Predict Immune Landscape, Chemotherapeutic Efficacy and Immunosuppressive Molecules in Hepatocellular Carcinoma. *BMC Cancer* 22, 229. doi:10.1186/s12885-022-09301-0
- Yu, G., Wang, L.-G., Han, Y., and He, Q.-Y. (2012). clusterProfiler: an R Package for Comparing Biological Themes Among Gene Clusters. *OMICS: A J. Integr. Biol.* 16, 284–287. doi:10.1089/omi.2011.0118
- Zhang, C., Zhao, X., Du, W., Shen, J., Li, S., Li, Z., et al. (2020). Ran Promotes the Proliferation and Migration Ability of Head and Neck Squamous Cell Carcinoma Cells. *Pathol. - Res. Pract.* 216, 152951. doi:10.1016/j.prp.2020.152951
- Zhang, H., Liu, R., Sun, L., Guo, W., and Hu, X. (2021). The Effect of Ferroptosis-Related Genes on Prognosis and Tumor Mutational Burden in Hepatocellular Carcinoma. *J. Oncol.* 2021, 1–12. doi:10.1155/2021/7391560

Conflict of Interest: The authors declare that the research was conducted in the absence of any commercial or financial relationships that could be construed as a potential conflict of interest.

Publisher's Note: All claims expressed in this article are solely those of the authors and do not necessarily represent those of their affiliated organizations, or those of the publisher, the editors, and the reviewers. Any product that may be evaluated in this article, or claim that may be made by its manufacturer, is not guaranteed or endorsed by the publisher.

Copyright © 2022 Li, Liu, Zhang, Gu and Zhao. This is an open-access article distributed under the terms of the Creative Commons Attribution License (CC BY). The use, distribution or reproduction in other forums is permitted, provided the original author(s) and the copyright owner(s) are credited and that the original publication in this journal is cited, in accordance with accepted academic practice. No use, distribution or reproduction is permitted which does not comply with these terms.